

Spin transport of indirect excitons in GaAs coupled quantum wells

J.R. Leonard,¹ Sen Yang,¹ L.V. Butov,¹ and A.C. Gossard²

¹Department of Physics, University of California at San Diego, La Jolla, CA 92093-0319

²Materials Department, University of California at Santa Barbara, Santa Barbara, California 93106-5050

(Dated: November 26, 2008)

Spin transport of indirect excitons in GaAs/AlGaAs coupled quantum wells was observed by measuring the spatially resolved circular polarization of the exciton emission. The exciton spin transport originates from the long spin relaxation time and long lifetime of the indirect excitons.

PACS numbers: 73.63.Hs, 78.67.De

Spin physics in semiconductors includes a number of interesting phenomena in electron transport, such as current-induced spin orientation (the spin Hall effect) [1, 2, 3], spin-induced contribution to the current [4], spin injection [5], and spin diffusion and drag [6, 7, 8, 9]. Besides the fundamental spin physics, there is also considerable interest in developing semiconductor electronic devices based on spin transport, which may offer advantages in dissipation, size and speed over charge-based devices, see [10, 11] and references therein.

Optical methods have been used as a tool for precise probe and control of electron spin via photon polarization and, in particular, for studying electron spin transport in semiconductors [10, 11, 12]. Excitons play a major role in the optical properties of quantum wells (QW) near the fundamental absorption edge. The spin dynamics of excitons in GaAs/AlGaAs single QW was extensively studied in the past, see [13, 14] and references therein. It was found that the spin relaxation time of the excitons in single QW is typically limited by the electron-hole exchange interaction and is short, on the order of a few tens of ps. Because of the short spin relaxation time, no spin transport of excitons was observed in single GaAs QWs.

Here, we report on the spin transport of indirect excitons in GaAs coupled quantum wells (CQW). The spin relaxation time of the indirect excitons is orders of magnitude longer than for regular excitons in single QW. In combination with the long lifetime of the indirect excitons, this makes possible the spin transport of the indirect excitons over substantial distances (up to several microns in the present work).

The spin dynamics of an exciton is related to the spin dynamics of its constituents - an electron and a hole [13, 14, 15]. The σ^+ (σ^-) polarized light propagating along the z -axis creates a heavy hole exciton with the electron spin state $s_z = -1/2$ ($s_z = +1/2$) and hole spin state $m_h = +3/2$ ($m_h = -3/2$) in GaAs QW structures. Then the exciton spin $S_z = s_z + m_h$ can be changed by flipping the spin of either the electron or the hole or by simultaneous flipping the spin of both electron and hole. In high-quality samples with a small concentration of magnetic impurities, the electron spin relaxation is typically

determined by the Dyakonov-Perel [16] mechanism. The hole spin relaxation in GaAs structures is typically determined by the hole momentum relaxation because a valence state is a mixture of the z -components of the $3/2$ spin [17]. The exciton spin relaxation by simultaneous flipping the spin of both electron and hole is driven by the electron-hole exchange interaction [13, 14, 15].

Heavy hole excitons with $S_z = +1$ (-1) emit σ^+ (σ^-) polarized light while excitons with $S_z = \pm 2$ are optically inactive. The dynamics of the polarization of the exciton emission $P = (I_+ - I_-)/(I_+ + I_-)$ is determined by the recombination and spin relaxation processes. For an optically active heavy hole exciton with spin $S_z = \pm 1$, spin flip of either electron or hole would transform the exciton to an optically inactive state with spin $S_z = \pm 2$, Fig. 1a. Therefore, these processes do not cause the decay of the emission polarization. The polarization decays when both the electron and hole flip their spins. This occurs in the two-step process due to the separate electron and hole spin flips and the single-step process due to the simultaneous flipping the spin of both electron and hole. The rate equations describing these processes [13, 14] yield the polarization of the exciton emission $P = \tau_p/(\tau_p + \tau_r)$, where $\tau_p^{-1} = 2(\tau_e + \tau_h)^{-1} + \tau_{ex}^{-1}$ is the relaxation time of the emission polarization, τ_{ex} is time for exciton flipping between $S_z = \pm 1$, τ_e and τ_h are electron and hole spin flip times, and τ_r is the exciton recombination time (for the typical case when the energy splitting between $S_z = \pm 1$ and $S_z = \pm 2$ states due to the electron-hole exchange interaction is smaller than $k_B T$).

In GaAs single QW, τ_h and τ_{ex} are typically short, in the range of several tens of ps, while τ_e can reach tens and hundreds of ns in high-quality samples. It is the long electron spin relaxation time, which makes possible the spin transport of electrons over large distances, see [6, 8, 9, 10, 11]. For $\tau_e \gg \tau_h, \tau_{ex}$, which is typical of GaAs single QW, $\tau_p \approx \tau_{ex}$ and, therefore, the small τ_{ex} results in a fast depolarization of the exciton emission within tens of ps [13, 14]. However, τ_{ex} is determined by the strength of the exchange Coulomb interaction between the electron and hole and is inversely proportional to the electron-hole overlap. This gives an opportunity to control the depolarization rate by changing the electron-

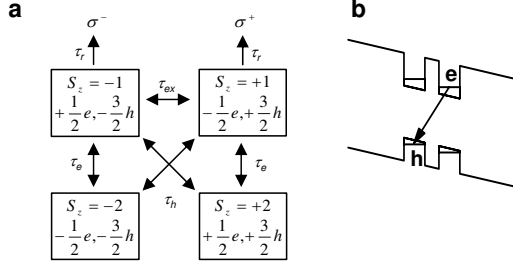


FIG. 1: (a) Exciton spin diagram, see text. (b) Energy diagram of the CQW structure; e, electron; h, hole.

hole overlap, e.g. in QW structures with different QW widths or with an applied electric field [13, 14].

The electron-hole overlap is drastically reduced in CQW structures. An indirect exciton in CQW is composed of an electron and a hole confined in spatially separated quantum wells, Fig. 1b. The spatial separation results in a small electron-hole overlap. One of the results of such small electron-hole overlap is a long exciton recombination time τ_r , which is typically in the range between tens of ns to tens of μ s [18, 19, 20], orders of magnitude longer than τ_r in single QW, which is typically in the range of tens and hundreds of ps [13, 14]. The long lifetimes of the indirect excitons make possible their transport over large distances, which can reach tens and hundreds of microns [21, 22, 23, 24, 25, 26]. The small electron-hole overlap for the indirect excitons should also result in a large τ_{ex} and, in turn, τ_p , thus making possible the exciton spin transport over large distances.

We probed exciton spin transport in a GaAs/AlGaAs CQW structure. Two 8 nm GaAs QW were separated by a 4 nm $\text{Al}_{0.33}\text{Ga}_{0.67}\text{As}$ barrier and surrounded by 200 nm $\text{Al}_{0.33}\text{Ga}_{0.67}\text{As}$ layers (see sample details in [20] where the same sample was studied). The electric field across the sample was controlled by an applied gate voltage V_g . The excitons were photoexcited by a cw 633 nm HeNe laser or tunable Ti:Sapphire laser focused to a spot $\sim 5\mu\text{m}$ in diameter. The excitation was circularly polarized (σ^+). The emission images in σ^+ and σ^- polarizations were taken by a CCD with an interference filter 800 ± 5 nm, which covers the spectral range of the indirect excitons. The spatial resolution was 1.4 micron. The spectra were measured using a spectrometer with resolution 0.3 meV.

Figure 2a shows the photoluminescence excitation (PLE) spectrum and polarization-resolved photoluminescence (PL) spectra of the indirect excitons. PLE reveals two peaks in the exciton absorption which correspond to the heavy-hole (hh) and light-hole (lh) direct excitons. The emission of the hh indirect exciton is observed at an energy below the hh direct exciton by $\sim eF_z d$, where F_z is the electric field and d is the distance be-

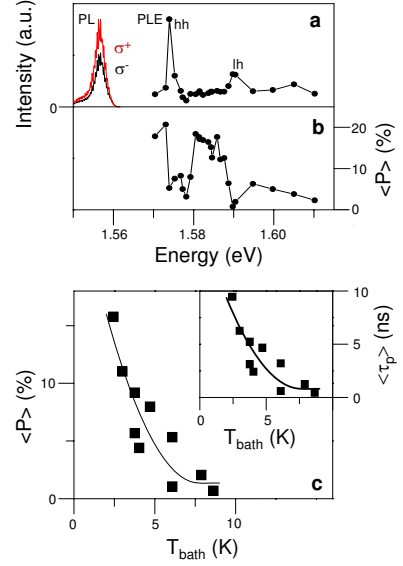


FIG. 2: (a) PLE spectrum and polarization resolved PL spectra of indirect excitons. (b) Spatially and spectrally averaged PL polarization of indirect excitons $\langle P \rangle$; $V_g = -1.1$ V, $T_{\text{bath}} = 1.7$ K, $P_{\text{ex}} = 5\mu\text{W}$, PL is measured with laser excitation energy $E_{\text{ex}} = 1.573$ eV. (c) $\langle P \rangle$ and (inset) the polarization relaxation time $\langle \tau_p \rangle = \langle \tau_r \rangle \langle P \rangle / (1 - \langle P \rangle)$ as a function of T_{bath} ; $V_g = -1.4$ V, $P_{\text{ex}} = 10\mu\text{W}$, and $E_{\text{ex}} = 1.572$ eV.

tween the electron and hole layers in CQW (corrections due to the interaction are described in [27]). Figure 2b shows degree of the circular polarization of PL of indirect excitons. No polarization was observed at strongly nonresonant excitation by HeNe laser ~ 400 meV above the indirect exciton. However, a substantial polarization of PL of indirect excitons was observed when the excitation was close to the hh direct exciton (Fig. 2b) at low temperatures (Fig. 2c). The polarization is reduced when the lh exciton (with $m_h = \pm 1/2$) is excited (Fig. 2a,b), consistent with the data in Ref. [28] and related to increased spin phase space (e.g. for the exciton with $s_z = +1/2$ and $m_h = +1/2$ the hole spin relaxation $m_h = +1/2 \rightarrow m_h = -3/2$ changes the emission polarization from σ^+ to σ^-).

The measured degree of the circular polarization P (Fig. 2c) and the measured exciton lifetime τ_r [20] give an opportunity for estimating the polarization relaxation time τ_p using the rate equations [13, 14], which result to $\tau_p = \tau_r P / (1 - P)$. The estimate for τ_p is presented in the inset to Fig. 2c (the dependence of τ_r on parameters, such as temperature in Fig. 2 and excitation power in Fig. 4, is taken into account in the estimates). The depolarization time of the emission of indirect excitons reaches 10 ns (Fig. 2c), orders of magnitude higher than that of the direct excitons in single QW [13, 14]. The depolarization time of the emission of indirect excitons τ_p is comparable

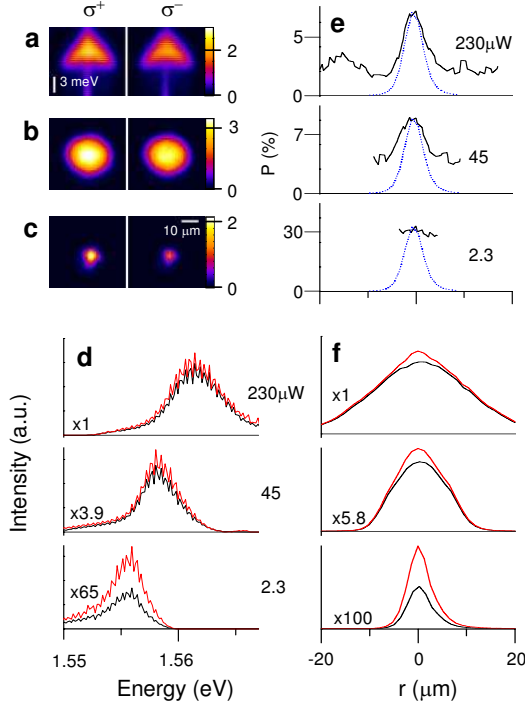


FIG. 3: (a) Energy- x images of the PL intensity of indirect excitons in σ^+ and σ^- polarizations; $V_g = -1.1$ V, $E_{ex} = 1.572$ eV, $P_{ex} = 140 \mu W$. $x - y$ images of the PL intensity of indirect excitons in σ^+ and σ^- polarizations for (b) $P_{ex} = 15 \mu W$ and (c) $P_{ex} = 4.7 \mu W$; $V_g = -1.1$ V, $E_{ex} = 1.582$ eV. (d) PL spectra of indirect excitons at the center of the exciton cloud ($r = 0$) in σ^+ (red) and σ^- (black) polarizations. The estimated exciton density at $r = 0$ for $P_{ex} = 2.3 \mu W$, $45 \mu W$, and $230 \mu W$ is $9 \cdot 10^8$, $2 \cdot 10^{10}$, and $4 \cdot 10^{10} cm^{-2}$, respectively. The density estimation is described in the text. $E_{ex} = 1.572$ eV. (e) PL polarization as a function of r for the same P_{ex} as in (d). The profile of the bulk emission, which presents the excitation profile, is shown by dotted lines. (f) PL intensity of indirect excitons in σ^+ (red) and σ^- (black) polarizations as a function of r for the same P_{ex} as in (d,e). $T_{bath} = 1.7$ K.

to their lifetime τ_r , which is in the range of tens of ns [20].

Characteristic polarization-resolved energy- x and $x-y$ images are shown in Fig. 3a-c. Figure 3d shows the density dependence of the spectra of the indirect excitons at the center of the exciton cloud in σ^+ and σ^- polarizations. The polarization and estimate for the polarization relaxation time is shown in Figs. 4a,b. The exciton density n was estimated from the energy shift δE as $n = \epsilon \delta E / (4\pi e^2 d)$ [25] (note that a higher estimate for n was suggested in Ref. [29]). The polarization degree of the exciton emission (Figs. 3d, 4a) and the polarization relaxation time (Fig. 4b) reduce with increasing density. (Note that no increase of P with n such as reported in Ref. [22] was observed in the present experiments.) Note also that this density dependence is consistent with the observed reduction of polarization when the excita-

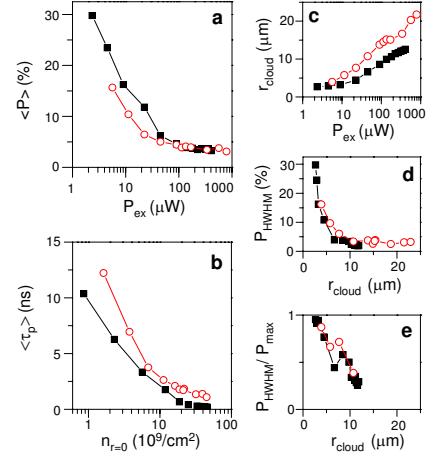


FIG. 4: (a) Spatially and spectrally averaged PL polarization as a function of excitation power. (b) Spatially and spectrally averaged polarization relaxation time as a function of density. (c) HWHM of the cloud of indirect excitons r_{cloud} as a function of excitation power. (d) Polarization at the HWHM of the exciton cloud P_{HWHM} as a function of r_{cloud} . (e) P_{HWHM}/P_{max} as a function of r_{cloud} . $V_g = -1.1$ V (squares), -1.6 V (circles). $T_{bath} = 1.7$ K.

tion energy corresponds to hh exciton, 1.572 eV, where an increased absorption results in a high density (Fig. 1b).

The increase of applied gate voltage $|V_g|$ results in the reduction of the electron-hole overlap and, in turn, increase of both τ_r and τ_{ex} . The former was measured in Ref. [20] for the sample. The polarization $P = \tau_p / (\tau_p + \tau_r)$ reduces with reducing electron-hole overlap (i.e. at higher $|V_g|$), see the data for $V_g = -1.1$ and -1.6 V in Fig. 4a. Such dependence indicates a slower increase of τ_p than τ_r with increasing $|V_g|$. This is consistent with the saturation of τ_p in the limit of vanishing electron-hole overlap where τ_{ex} becomes large compared to τ_e and τ_h so that $\tau_p^{-1} = 2(\tau_e + \tau_h)^{-1} + \tau_{ex}^{-1}$ is determined by τ_e , for which no substantial dependence on the electron-hole overlap is expected [13, 14]. (This is also consistent with the fact that essentially no polarization of the emission of the indirect excitons was observed in another studied GaAs/AlGaAs CQW sample with 15 nm QWs; in this sample, the larger separation between the electron and hole layers results to a much smaller electron-hole overlap, as revealed by a considerably longer τ_r , in the range of several μs .) Figure 4b indicates that $\tau_p = \tau_r P / (1 - P)$ still increases with reducing electron-hole overlap (i.e. at higher $|V_g|$).

The radius of the exciton cloud is essentially equal to the excitation spot radius at low densities and increases at high densities, Figs. 3b, c, f, 4c. Such behavior was observed earlier and attributed to the exciton localization due to in-plane disorder at low densities and exciton delocalization and transport away from the excitation spot

at high exciton densities when the disorder is screened by the repulsive interaction between the indirect excitons [23, 25]. Previous studies indicate that in this range of temperatures and densities, exciton transport in the CQW structure can be described by drift and diffusion [25].

Figures 3f and 3e show the polarization-resolved PL intensity and polarization P , respectively, as a function of distance from the center of the laser excitation spot. The polarization at the half-width-half-maximum (HWHM) of the exciton cloud P_{HWHM} (Fig. 4d) and the ratio P_{HWHM}/P_{max} (Fig. 4e) show that the polarization is observed up to several microns away from the origin which gives the length scale for the exciton spin transport in the structure. This length scale is large enough to allow studying the basic properties of the exciton spin transport by the optical experiments (it is beyond the diffraction-limited spatial resolution, which is 1.4 microns in the present work). It is also large enough to allow studying spin-polarized exciton gases in microscopic patterned devices, e.g. in in-plane lattices [30], which period can be below a micron. Furthermore, the length scale for exciton spin transport is comparable to the scale of the excitonic devices such as the excitonic transistors and circuits [31, 32] (the distance between source and drain for an excitonic transistor was $3\text{ }\mu\text{m}$ in Refs. [31, 32]; however, it is expected that the dimensions can be reduced below $1\text{ }\mu\text{m}$ by using e-beam lithography). This may allow creating spin-optoelectronic devices where the spin fluxes of excitons will be controlled in analogy to the control of the fluxes of unpolarized excitons in Refs. [31, 32].

A quick reduction of the polarization is observed in the vicinity of the excitation spot, followed by the tail with a weak spatial dependence, Fig. 3e,f. Since the lifetime τ_r and polarization relaxation time τ_p of the indirect excitons are comparable, the quick reduction of the polarization on a length scale smaller than the diffusion length ($\sqrt{D_s\tau_p} < \sqrt{D\tau_r}$) indicates that the exciton spin diffusion coefficient D_s near $r = 0$ is smaller than the exciton diffusion coefficient D . Note parenthetically that in the case of electron transport, the spin Coulomb drag results to a smaller value of D_s compared to D [7, 8]. Note also that the exciton temperature is higher in the vicinity of the excitation spot [25] and this contributes to a quicker reduction of the polarization there according to the temperature dependence in Fig. 2c. Theory of spin relaxation and transport of indirect excitons, which can be compared to the experimental data, has yet to be developed.

In conclusion, the spatially resolved circular polarization of the emission of long-life indirect excitons in CQW structures was studied. The polarization relaxation time of the emission of the indirect excitons exceeds that of regular direct excitons by orders of mag-

nitude and reaches ten ns. The polarization degree and the polarization relaxation time reduce with increasing density and temperature. Spin transport of the indirect excitons was observed. The exciton spin transport originates from the long spin relaxation time and long lifetime of the indirect excitons.

This work is supported by DOE. We thank Misha Fogler, Lu Sham, and Congjun Wu for discussions.

-
- [1] M.I. Dyakonov and V.I. Perel', Phys. Lett. A **35**, 459 (1971).
 - [2] J.E. Hirsch, Phys. Rev. Lett. **83**, 1834 (1999).
 - [3] V. Sih, R.C. Myers, Y.K. Kato, W.H. Lau, A.C. Gossard and D.D. Awschalom, Nature Phys. **1**, 31 (2005)
 - [4] M.I. Dyakonov and V.I. Perel', Zh. Eksp. Teor. Fiz. Pis'ma Red. **13**, 657 (1971) [Sov. Phys. JETP Lett. **13**, 467 (1971)].
 - [5] A.G. Aronov and G.E. Pikus, Fiz. Tekh. Poluprovodn. **10**, 1177 (1976) [Sov. Phys. Semicond. **10**, 698 (1976)].
 - [6] J. M. Kikkawa and D. D. Awschalom, Nature **397**, 139 (1999).
 - [7] I. D'Amico and G. Vignale, Europhys. Lett. **55**, 566 (2001).
 - [8] C. P. Weber, N. Gedik, J. E. Moore, J. Orenstein, J. Stephens, and D. D. Awschalom, Nature **437**, 1330 (2005).
 - [9] S.G. Carter, Z. Chen, and S.T. Cundiff, Phys. Rev. Lett. **97**, 136602 (2006).
 - [10] S.A. Wolf, D.D. Awschalom, R.A. Buhrman, J.M. Daughton, S. von Molnár, M.L. Roukes, A.Y. Chtchelkanova, D.M. Treger, Science **294**, 1488 (2000).
 - [11] D.D. Awschalom and M.E. Flatté, Nature Phys. **3**, 153 (2007).
 - [12] T.H. Stievater, Xiaoqin Li, D.G. Steel, D. Gammon, D.S. Katzer, D. Park, C. Piermarocchi, and L.J. Sham, Phys. Rev. Lett. **87**, 133603 (2001).
 - [13] M.Z. Maialle, E.A. de Andrada e Silva, and L.J. Sham, Phys. Rev. B **47**, 15776 (1993).
 - [14] A. Vinattieri, Jagdeep Shah, T.C. Damen, D.S. Kim, L.N. Pfeiffer, M.Z. Maialle, and L.J. Sham, Phys. Rev. B **50**, 10868 (1994).
 - [15] L.C. Andreani and F. Bassani, Phys. Rev. B **41**, 7536 (1990).
 - [16] M.I. Dyakonov and V.I. Perel, Zh. Eksp. Teor. Fiz. **60**, 1954 (1971) [Sov. Phys. JETP **33**, 1053 (1971)].
 - [17] T. Uenoyama and L.J. Sham, Phys. Rev. B **42**, 7114 (1990).
 - [18] A. Alexandrou, J. A. Kash, E. E. Mendez, M. Zachau, J. M. Hong, T. Fukuzawa, and Y. Hase, Phys. Rev. B **42**, 9225 (1990).
 - [19] A. Zrenner, P. Leeb, J. Schäfler, G. Böhm, G. Weimann, J. M. Worlock, L. T. Florez, and J. P. Harbison, Surf. Sci. **263**, 496 (1992).
 - [20] L.V. Butov, A. Imamoglu, A.V. Mintsev, K.L. Campman, and A.C. Gossard, Phys. Rev. B **59**, 1625 (1999).
 - [21] M. Hagn, A. Zrenner, G. Böhm, G. Weimann, Appl. Phys. Lett. **67**, 232 (1995).
 - [22] A.V. Larionov, V.B. Timofeev, J. Hvam, K. Soerensen, Zh. Eksp. Teor. Fiz. **117**, 1255 (2000) [JETP **90**, 1093 (2000)].
 - [23] L.V. Butov, A.C. Gossard, D.S. Chemla, Nature **418**, 751 (2002).
 - [24] Z. Vörös, R. Balili, D.W. Snoke, L. Pfeiffer, K. West, Phys. Rev. Lett. **94**, 226401 (2005).
 - [25] A.L. Ivanov, L.E. Smallwood, A.T. Hammack, Sen Yang, L.V. Butov, A.C. Gossard, Europhys. Lett. **73**, 920 (2006).

- [26] A. Gärtner, A.W. Holleithner, J.P. Kotthaus, D. Schul, Appl. Phys Lett. **89**, 052108 (2006).
- [27] L.V. Butov, A.A. Shashkin, V.T. Dolgoplov, K.L. Campman, and A.C. Gossard, Phys. Rev. B **60**, 8753 (1999).
- [28] T.C. Damen, Luis Viña, J.E. Cunningham, Jagdeep Shah, and L.J. Sham, Phys. Rev. Lett. **67**, 3432 (1991).
- [29] C. Schindler and R. Zimmermann, Phys. Rev. B **78**, 045313 (2008).
- [30] A.T. Hammack, N.A. Gippius, Sen Yang, G.O. Andreev, L.V. Butov, M. Hanson, A.C. Gossard, J. Appl. Phys. **99**, 066104 (2006).
- [31] A.A. High, A.T. Hammack, L.V. Butov, M. Hanson, and A.C. Gossard, Opt. Lett. **32**, 2466 (2007).
- [32] A.A. High, E.E. Novitskaya, L.V. Butov, M. Hanson, and A.C. Gossard, Science **321**, 229 (2008).